

## Computational study of CO<sub>2</sub> solubility in amino acid-based ionic liquids using COSMO-RS

SULafa Abdalmageed Saadaldeen Mohammed<sup>1,a</sup>,  
WAN ZAIREEN NISA Yahya<sup>1,2,b\*</sup>, MOHAMAD AZMI Bustam<sup>1,2,c</sup>,  
AMIN Abbasi<sup>1,d</sup> and MD GOLAM Kibria<sup>3,e</sup>

<sup>1</sup>Chemical Engineering Department, Universiti Teknologi PETRONAS, 32610 Seri Iskandar, Perak, Malaysia

<sup>2</sup>Centre of Research in Ionic Liquids, Universiti Teknologi PETRONAS, 32610 Seri Iskandar, Perak, Malaysia

<sup>3</sup>Chemical and Petroleum Engineering, University of Calgary, Alberta, Canada, 2500 University Drive, NW, Calgary, Alberta, T2N 1N4, Canada

<sup>a</sup>sulafa\_19001261@utp.edu.my, <sup>b</sup>zaireen.yahya@utp.edu.my, <sup>c</sup>azmibustam@utp.edu.my,  
<sup>d</sup>amin\_18000407@utp.edu.my, <sup>e</sup>md.kibria@ucalgary.ca

**Keywords:** Ionic Liquid, Amino Acid, CO<sub>2</sub> Solubility, COSMO-RS

**Abstract.** The carbon capture, use, and sequestration (CCUS) techniques are proven to be efficient at lowering the atmospheric concentration of carbon dioxide. Notwithstanding the advances in this area, there are still significant restrictions in carbon dioxide (CO<sub>2</sub>) capture techniques in industry such as high capital costs, solvent evaporation losses, and low absorption and desorption rates. Ionic liquids (ILs) have received much interest as green solvent due to the benefits of their distinctive properties such as low vapor pressure and their capacity to capture CO<sub>2</sub> making them a suitable replacement for present solvents, such as amines. Amino acid based ILs having close similarity with the alkanolamines may potentially have high affinity for CO<sub>2</sub> absorption. Nevertheless, available database on these ILs is still limited and only focus on the common types of amino acids. Therefore, this paper aims to predict the CO<sub>2</sub> absorption of different amino acid-based ionic liquids as cation/anion using quantum chemical calculation tools namely Conductor like Screening Model for Real Solvents (COSMO-RS) and TURBOMOLE. We evaluated 84 different ILs of different cations and anions based on their CO<sub>2</sub> capacity, activity coefficient at infinite dilution ( $\gamma^\infty$ ), and Henry's constant (H). The results showed that amino acid as anions significantly enhanced the CO<sub>2</sub> solubility compared to amino acid as cations. However, glycinium tetrafluoroborate [Gly<sup>+</sup>][BF<sub>4</sub><sup>-</sup>] showed high affinity for CO<sub>2</sub> absorption compared to other amino acid-cations based with activity coefficient at infinite dilution ( $\gamma^\infty$ ) = 0.117 and (H) = 8.07. We showed that the selection of anions/cations can significantly change the CO<sub>2</sub> capacity in ILs.

### Introduction

The concentration of CO<sub>2</sub> in the atmosphere increases over time because of carbon emissions from the burning of fossil fuels [1]. One successful strategy to reduce CO<sub>2</sub> emissions in the atmosphere is by carbon dioxide capture, utilization, and storage (CCUS) [2]. Many industries currently use the amine scrubbing technique as their primary CO<sub>2</sub> capture technology [3, 4]. This process however, have numerous weaknesses such as equipment corrosion, high energy need for regeneration, solvent loss, and oxidative degradation [5]. Ionic liquids (ILs) are promising for CO<sub>2</sub> capture because of their strong affinity for acid gases [6], high physical and chemical stability [7], low vapor pressure [8], and strong polarity [9]. Moreover, the structures of ILs (cation and/or anion) can be finely tuned to enhance their physical and chemical characteristics.

CO<sub>2</sub> absorption in non-functionalized ILs mainly takes place by physical absorption through weak Lewis acid–base interactions [10]. Subsequently, the amine-functionalization of the cation and/or anion of the ILs have been investigated since amine solvents showed strong reactivity with CO<sub>2</sub> molecules [11, 12]. Similarly, amino acid can also be utilized as cation or anion to enhance the efficiency of CO<sub>2</sub> absorption in ILs [13]. Amino acids contain a primary amine (–NH<sub>2</sub>) and carboxyl group (–COOH), thus, the reactivity of CO<sub>2</sub> with amino acids is expected to be similar as that of alkanolamines [14, 15]. However, there is still a conflict on the actual mechanism of the CO<sub>2</sub> reaction with amino acids [16].

Shahrom et al. [13] studied eight ionic liquids that consist of amino acids-based anions namely lysine [Lys], proline [Pro], histidine [His], serine [Ser], taurine [Tau], alanine [Ala], arginine [Arg], and glycine [Gly]) with vinylbenzyltrimethylammonium [VBTMA] as cation. They reported that [Arg] and [Lys] showed the highest CO<sub>2</sub> sorption values followed by [His], [Ser], [Tau], [Pro], [Gly], and [Ala]. Another study by Sistla and Khanna [10] evaluated different amino acid based ILs and observed that amine-anion ILs perform better than amino-cation and non-functionalized ILs. In their study, 1-butyl-3-methylimidazolium [BMIM] was used as the cation and found that the order of CO<sub>2</sub> capacity in the ILs starting from the highest is [Arg]>[Lys]>[His]>Methionine [Met]> Leucine [Leu] >[Gly]> Valine [Val]>[Ala]>[Pro]. They explained it by the availability of more accessible amine (N) groups. Noorani and Mehrdad [1] also studied the CO<sub>2</sub> solubility in 1-butyl-3-methylimidazolium glycine [BMIM][Gly], [BMIM][Ala], and [BMIM][Val], where they reported that the order of CO<sub>2</sub> capacity starting from the highest is [BMIM][Gly]>[BMIM][Ala]>[BMIM][Val].

The solubility of CO<sub>2</sub> in amino acid-based ILs are therefore a subject of interest for further investigation. However, the current database on these ILs is still limited, mainly experimental based, and only focused on the common types of amino acids. This aim of this study is to predict the CO<sub>2</sub> solubility of different amino acid-based ionic liquids as cation/anion and to provide better understanding of their respective roles using Conductor like Screening Model for Real Solvents (COSMO-RS). COSMO-RS is a quantum chemical calculation tool to estimate the chemical potential differences of molecules inside liquids designed by Klamt [17, 18]. The software has been used in various application for prediction of thermodynamic properties and behavior of ionic liquids [19]. The screening of ILs via COSMO-RS will aid in the design for the desired ILs for CO<sub>2</sub> capture and avoid uncertain trails.

## Methods

Initially, to generate COSMO files, the molecular structures of ILs (cations/anions) were built based on density functional theory using Turbomole software (TmoleX). For TmoleX settings, BP functional with triple-zeta valence polarized set (BP\_TZVP\_C30\_1301) was used as parameterization for COSMO-RS calculations. The sigma ( $\sigma$ ) profile and sigma ( $\sigma$ ) surface were generated. The  $\sigma$ -profile of any molecule is calculated based on the weighted sum of the profiles of all segments [17] as per Equation (1);

$$p_i(\sigma) = \sum_i^N x_i \times p_i \quad (1)$$

where  $x_i$  is the mole fraction of component (i) in the mixture and  $p_i$  is the  $\sigma$  profile of any molecule X. The Henry constant (H) is a significant indication of gas solubility, which is directly proportional to the activity coefficient. A low value of H is an indication of good CO<sub>2</sub> solubility. The Henry's constant values for selected ILs were calculated using Equation (2);

$$H_s^i = \gamma_s^{S,\infty} \times P_s^i \quad (2)$$

where,  $\gamma_s^{S,\infty}$  is the activity coefficient at infinite dilution and  $P_s^i$  is the vapor pressure.

To evaluate the effect of anions and cations functionalization, the activity coefficient at infinite dilution ( $\gamma^\infty$ ), CO<sub>2</sub> capacity (mole CO<sub>2</sub>/mole of ILs), and Henry's constant (H) of 84 ILs were

estimated using COSMO-RS for the solubility prediction. For this study, the ILs structures of the cations are: 1-butyl-3-methylimidazolium (BMIM), tetrabutylammonium (N4444), dibutylpyrrolidinium (BBPyrro), glycinium (Gly<sup>+</sup>), L-lysinium(+1) (Lys<sup>+</sup>), and (MGlyB) as depicted in Figure 1. The ILs structures of the anions are: tetrafluoroborate (BF<sub>4</sub>), bromide (Br), bis(trifluoromethane)sulfonimide (TFSI), nitrate (NO<sub>3</sub>), Gly, Ala, Val, Leu, isoleucine (Ile), phenylalanine (Phe), Pro, serine (Ser), threonine (Thr), tyrosine (Tyr), cysteine (Cys), Met, Lys, Arg, His, tryptophan (Trp), aspartic acid (Asp), glutamic acid (Glu), asparagine (Asn), and glutamine (Gln) as shown in Figure 2.

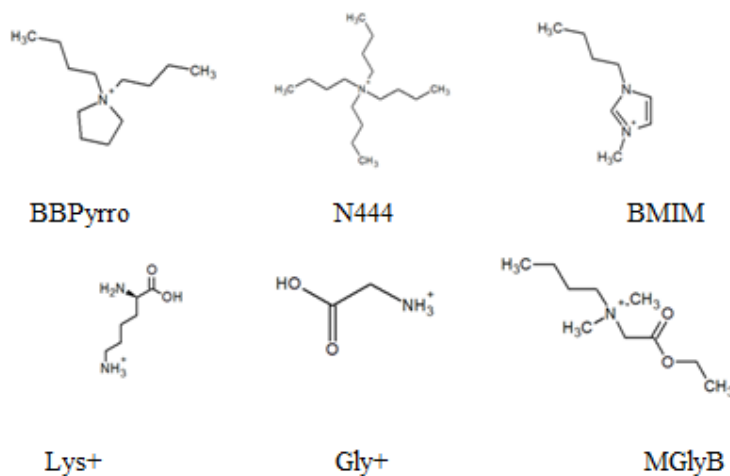
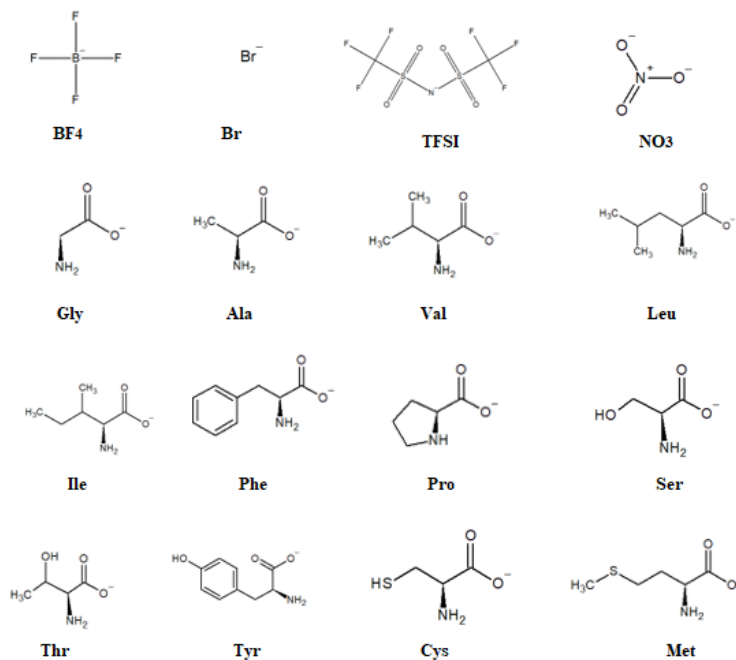


Fig. 1. Different cations structures of the ILs used in this study.



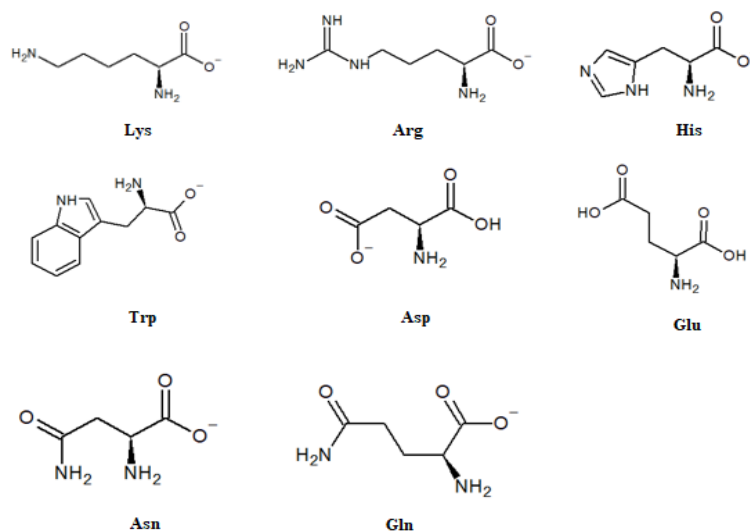


Fig. 2. Different anions structures of the ILs used in this study.

## Results and Discussions

To study the effect of amine functional group ( $-\text{NH}_2$ ) and carboxyl group ( $-\text{COOH}$ ) on the capacity of  $\text{CO}_2$  in ILs, different amine-anion ILs, non-functionalized ILs and, amino-cation ILs were evaluated. First, 20 amine-anion ILs with different combination of cations namely BMIM, BBPyrro, and N4444 were evaluated to study the effect of amino acid based-anion ILs on  $\text{CO}_2$  capacity.

For BMIM-cation based ILs, the values of  $\text{CO}_2$  capacity are shown in Figure 3. It can be observed that the order of  $\text{CO}_2$  capacity starting from the highest is  $[\text{Arg}] > [\text{Lys}] > [\text{Met}] > [\text{Phe}] > [\text{His}] > [\text{Trp}] > [\text{Leu}] > [\text{Val}] > [\text{Asn}] > [\text{Gly}] > [\text{Ala}] > [\text{Pro}] > [\text{Ile}] > [\text{Cys}] > [\text{Ser}] > [\text{Gln}] > [\text{Tyr}] > [\text{Thr}] > [\text{Asp}] > [\text{Glu}]$ . Figure 4 shows the Henry's constant ( $H$ ) and activity coefficient at infinite dilution. It can be noted that the order of Henry's constant ( $H$ ) values starting from the lowest is  $[\text{Arg}] < [\text{Lys}] < [\text{Met}] < [\text{Phe}] < [\text{His}] < [\text{Trp}] < [\text{Leu}] < [\text{Val}] < [\text{Asn}] < [\text{Gly}] < [\text{Ala}] < [\text{Pro}] < [\text{Ile}] < [\text{Cys}] < [\text{Ser}] < [\text{Gln}] < [\text{Tyr}] < [\text{Thr}] < [\text{Asp}] < [\text{Glu}]$ . The trend observed is also generally consistent with the order obtained for  $\gamma^\infty$  as shown in Figure 4. By comparing  $\text{CO}_2$  capacity prediction with the experimental results obtained by Sistla and Khanna [10], almost similar trend with a slight difference was observed where  $[\text{Arg}]$  and  $[\text{Lys}]$  showed the highest  $\text{CO}_2$  capacity values while  $[\text{Ala}]$  and  $[\text{Pro}]$  showed the lowest values. The results of the overall 60 ILs screening, showed that  $[\text{Arg}]$  and  $[\text{Lys}]$  have the highest  $\text{CO}_2$  capacity, while  $[\text{Thr}]$ ,  $[\text{Asp}]$ , and  $[\text{Glu}]$  showed the lowest affinity for  $\text{CO}_2$  absorption.

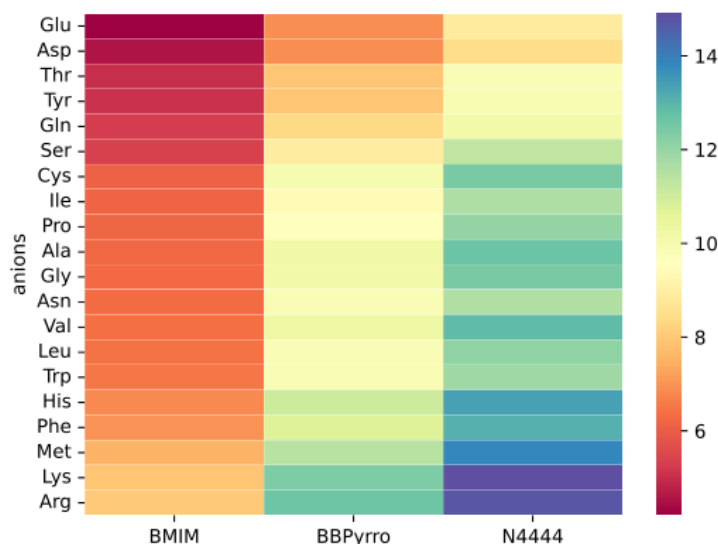


Fig. 3. CO<sub>2</sub> capacity values for different ILs, the red color represents the highest value followed by orange, yellow, green, and blue.

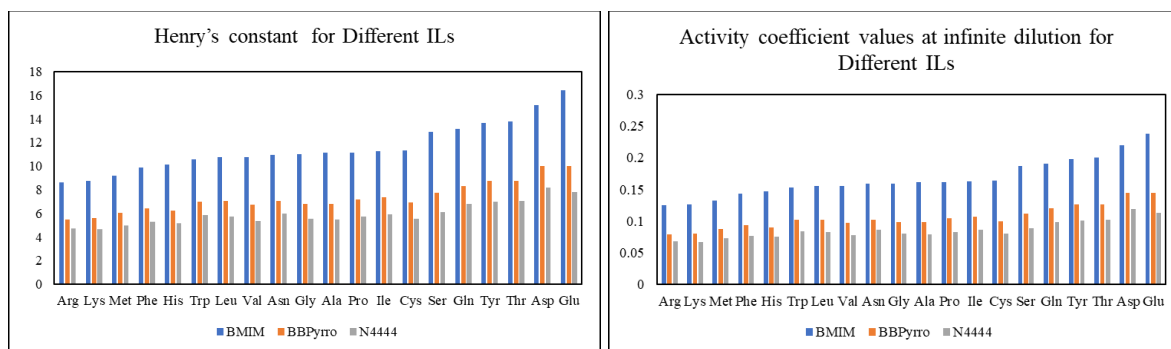


Fig. 4. Henry's constant ( $H$ ) values (left) and activity coefficient values ( $\gamma^\infty$ ) (right) for different ILs.

The  $\sigma$ -profile and  $\sigma$ -surface for CO<sub>2</sub>, [BMIM], [Arg], [Lys], [Thr], [Asp], and [Glu] are presented in Figure 5 to understand the effect of molecular structures on the activity performance. The  $\sigma$ -profile represents the charge density profiles for the structures, and it can be divided into three major parts: hydrogen bond donor for  $\sigma < -0.01 \text{ e}/\text{\AA}^2$ , hydrogen bond acceptor for  $\sigma > +0.01 \text{ e}/\text{\AA}^2$ , and nonpolar for  $-0.01 \text{ e}/\text{\AA}^2 < \sigma < +0.01 \text{ e}/\text{\AA}^2$ . Furthermore,  $\sigma$ -surface is used to estimate the charge distribution of the structure using color coded representation. The neutral characteristic is represented by green color, yellow color represents a partial negative charge while the strong electronegativity is represented by red color, and the blue color represents a strong positive charge. From Figure 5 it can be observed that [Arg] and [Lys] anions are highly nonpolar compared to [Thr], [Asp] and [Glu] anions, which increase the London dispersion interaction with the nonpolar CO<sub>2</sub>. Moreover, it can be noted that [Arg] and [Lys] anions have high hydrogen bond acceptance properties which increase the interaction with BMIM that has hydrogen bond donation property. On the other hand [Thr], [Asp], and [Glu] anions, have hydrogen bond donation properties compared to [Arg] and [Lys] anions, which reduce their attraction forces with BMIM as well as the attraction forces with CO<sub>2</sub> since CO<sub>2</sub> is relatively considered as acid.

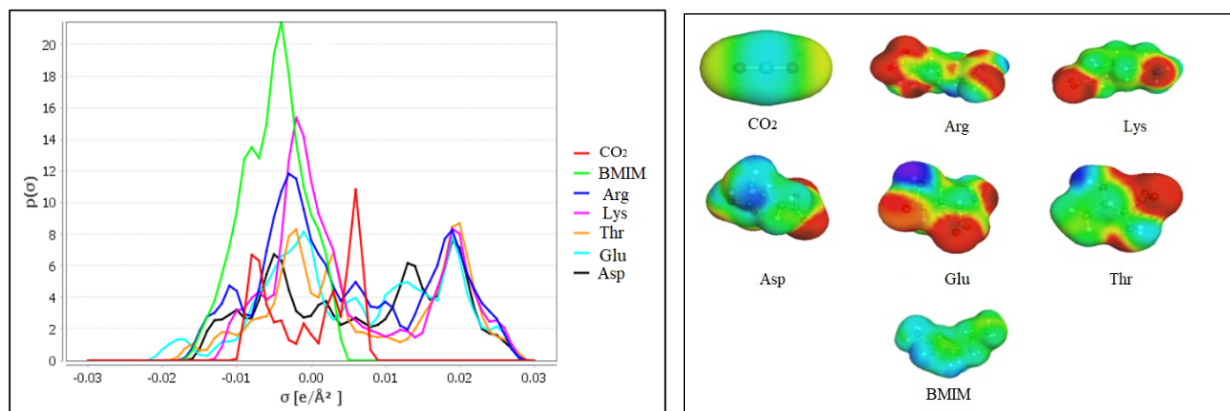


Fig.5 Sigma profile (left) and sigma surface (right) for CO<sub>2</sub>, [BMIM], [Arg], [Lys], [Thr], [Asp], and [Glu].

To understand the effect of different cations on CO<sub>2</sub> capacity, [N4444], and [BBPyrro] cations with the same 20 anions were further evaluated. The values of CO<sub>2</sub> capacity for N4444-based ILs and BBPyrro-based ILs are shown in Figure 3. For N4444-based ILs, the order of CO<sub>2</sub> capacity starting from the highest is [Lys]>[Arg]>[Met]>[His]>[Phe]>[Val]>[Ala]>[Cys]>[Gly]>[Leu]>[Pro]>[Trp]>[Ile]>[Asn]>[Ser]>[Gln]>[Tyr]>[Thr]>[Glu]>[Asp].

The result is consistent for the Henry's constant (H) values for N4444 as shown in Figure 4, from the lowest is [Lys]<[Arg]<[Met]<[His]<[Phe]<[Val]<[Ala]<[Cys]<[Gly]<[Leu]<[Pro]<[Trp]<[Ile]<[Asn]<[Ser]<[Gln]<[Tyr]<[Thr]<[Glu]<[Asp]. The same sequence was found for  $\gamma^\infty$  values as shown in Figure 4. By comparing the predicted CO<sub>2</sub> capacity with the experimental results obtained by Recker et al. [20], a similar trend was observed where [Val] showed higher CO<sub>2</sub> capacity than [Leu], followed by [Ile]. For BBpyrro-based ILs, the predicted CO<sub>2</sub> capacity sequence starting from the highest is [Arg]>[Lys]>[Met]>[His]>[Phe]>[Val]>[Ala]>[Gly]>[Cys]>[Trp]>[Asn]>[Leu]>[Pro]>[Ile]>[Ser]>[Gln]>[Tyr]>[Thr]>[Glu]>[Asp]. While for the order of H values starting from the lowest is [Arg]<[Lys]<[Met]<[His]<[Phe]<[Val]<[Ala]<[Gly]<[Cys]<[Trp]<[Asn]<[Leu]<[Pro]<[Ile]<[Asn]<[Ser]<[Gln]<[Tyr]<[Thr]<[Glu]<[Asp]. Similar trend was then observed for the for  $\gamma^\infty$  values as shown in Figure 4.

It can be clearly seen that the order of CO<sub>2</sub> capacity slightly varies by changing the cations. It can be noted that when comparing the three cations, ammonium [N4444]-based ILs recorded an overall higher CO<sub>2</sub> capacity than [BBPyrro] and [BMIM]. To investigate the cause of variation of CO<sub>2</sub> capacity order with different cations, the  $\sigma$ -profile for CO<sub>2</sub>, [BMIM], [N4444], and [BBpyrro] were generated as shown in Figure 6. From Figure 6, it can be observed that [N4444] is strongly nonpolar, followed by [BBPyrro] then [BMIM] which explains the high CO<sub>2</sub> affinity of [N4444] compared to [BBPyrro] and [BMIM].

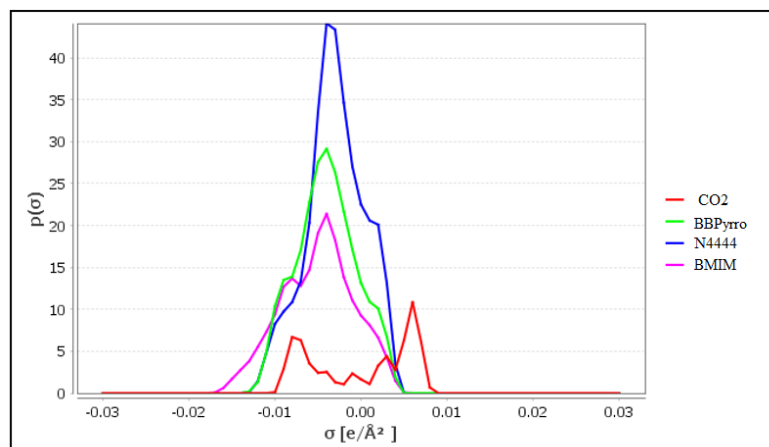


Fig. 6. Sigma profile for CO<sub>2</sub>, BBpyrro, N4444, and BMIM

To understand the effect of amine anions on the cations it is important to look at the nature of the amino acids. Amino acids (AAs) can be classified into five major groups based on the properties of the "R" group in each amino acid. First is AAs with polar uncharged side chain such as ([Ser], [Thr], [Asp], [Glu]), second is AAs with hydrophobic side like ([Ala],[Val], [Ile], [Leu], [Met], [Phe], [Tyr], [Trp]), third is AAs with basic side like ([His], [Arg], [Lys]), fourth is AA with acidic side like ([Glu], [Asp]), and fifth is AA with special cases ([Cys], [Gly], [Pro]).

For BBPyrro, N4444, and BMIM -based cations, the nonpolar anions with high hydrogen bond acceptance properties and less hydrogen bond donation properties (with base side chain) like [Arg] and [Lys] shows higher CO<sub>2</sub> capacity, while the anion with acidic properties like [Glu] and [Asp] showed the lowest values. This is because CO<sub>2</sub> is considered as nonpolar and relatively acid. For nonpolar cation [N4444], the nonpolar amino acid-based anion like [Lys] showed high affinity for CO<sub>2</sub> compared to the relatively polar [Arg]. On the other hand, the relatively polar cation like [BMIM] showed higher CO<sub>2</sub> capacity with the relatively polar [Arg] compared to the highly nonpolar anion [Lys].

To study the effect of cation-based amino acids on CO<sub>2</sub> capacity, glycinium [Gly<sup>+</sup>], L-lysinium(+1) [Lys<sup>+</sup>], and [MGlyB] cations were evaluated along with tetrabutylammonium [N4444], [BMIM] and [BBPyrro] with different anions. From Figure 7, it can be observed that for bromide based ILs, the CO<sub>2</sub> capacity order starting from the highest is [N4444]>[BBPyrro]>[BMIM]>[MGlyB]>[Lys<sup>+</sup>]>[Gly<sup>+</sup>]. From Figure 8, similar trend was observed for  $\gamma^\infty$  and H values starting from the lowest [N4444]<[BBPyrro]<[BMIM]<[MGlyB]<[Lys<sup>+</sup>]<[Gly<sup>+</sup>]. It can be noted that the cation-based amino acids generally have low CO<sub>2</sub> solubility. For further validation of the results, other common anions namely TFSI, BF<sub>4</sub> and NO<sub>3</sub> anion-based were evaluated with the same combinations of cations. From Figure 7 and Figure 8, it can be observed that TFSI and NO<sub>3</sub> anion-based showed the same trend as Br-based ILs. Interestingly, for BF<sub>4</sub> the order of CO<sub>2</sub> capacity starting from the highest is [N4444]>[BBPyrro]>[Gly<sup>+</sup>]>[BMIM]>[MGlyB]>[Lys<sup>+</sup>]. One striking trend is observed for the case of [Gly<sup>+</sup>] cations. According to the combination of anion, the CO<sub>2</sub> absorption vary significantly. It can be observed that [Gly<sup>+</sup>] cations showed highest affinity for CO<sub>2</sub> absorption when coupled with BF<sub>4</sub>.

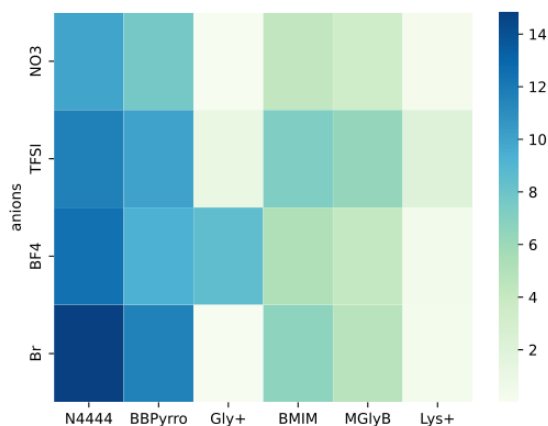


Fig. 7. CO<sub>2</sub> capacity values for different ILs, the red color represent the highest value followed by orange, yellow, and green.

		Anions				Anions			
		BF4	TFSI	NO3	Br	BF4	TFSI	NO3	Br
Cations	N4444	0.08012275	0.08593158	0.1003414	0.06747542	5.53	5.94	6.93	4.66
	BBPyrro	0.10701314	0.09972247	0.13052135	0.08603673	7.39	6.89	9.02	5.94
	Gly+	0.11682421	0.89772805	13.19474802	1263.34407176	8.07	62.01	911.5	8726.89
	BMIM	0.19396429	0.13791883	0.2356154	0.15027662	13.4	9.53	16.28	10.38
	MGlyB	0.24145579	0.15690728	0.29848708	0.21102923	16.7	10.84	20.62	14.58
	Lys+	2.44863768	0.46763114	3.74863892	3.10644848	169.15	32.3	258.5	214.59

Fig. 8. Henry's constant (*H*) values and infinite dilution activity coefficient ( $\gamma^\infty$ ) values for different ILs

To investigate the activity of [Gly<sup>+</sup>] cation with different anions, sigma profiles and sigma potential for [Gly<sup>+</sup>], [N4444], [BBPyrro], [BMIM], [MGlyB], [Lys<sup>+</sup>], [TFSI], [Br], [BF<sub>4</sub>] and [NO<sub>3</sub>] were generated as shown in Figure 9. From the sigma profile and sigma potential, it can be observed that [Gly<sup>+</sup>] has strong hydrogen bond donation property while BF<sub>4</sub> has strong hydrogen bond acceptance property which increases the molecular interaction between the molecules. It can also be noted that although Br anion is highly electronegative, [BF<sub>4</sub>] showed higher CO<sub>2</sub> capacity and this is due to branched chain of B-F in [BF<sub>4</sub>] that provides higher interaction surface especially with [Gly<sup>+</sup>] since glycine is classified among the special group because it contains a hydrogen at its side chain N<sup>+</sup>H<sub>3</sub> (rather than carbon as in all other amino acid), which makes the glycine the most flexible amino acid. It can be observed that the interaction between the CO<sub>2</sub> and big structures like [Lys<sup>+</sup>] and other cations is mainly by London dispersion interaction (nonpolar-nonpolar) interaction due to the distance from the charged atoms unlike [Gly<sup>+</sup>]. It can be therefore deduced that the cations/anions combination play important roles on CO<sub>2</sub> capacity in ILs through the molecular interaction.



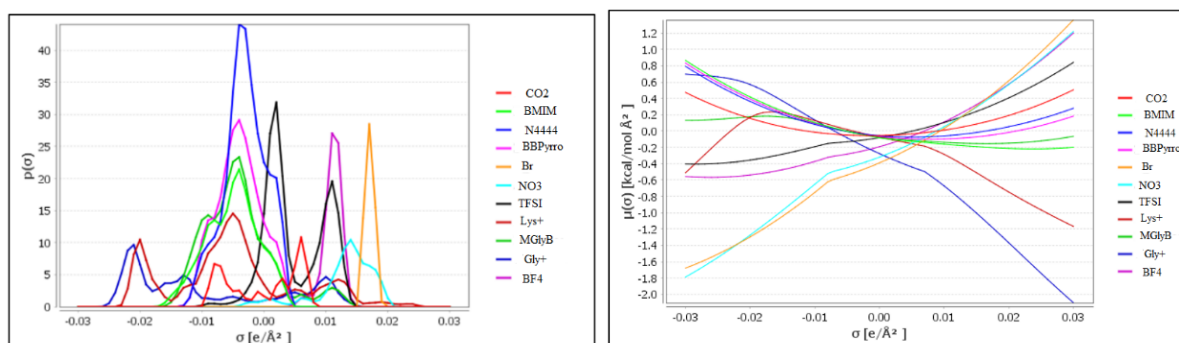


Fig. 9. Sigma profile (left) and sigma potential (right) for different anions and cations

## Conclusion

The effect of amine functional group ( $-\text{NH}_2$ ) and carboxyl group ( $-\text{COOH}$ ) on  $\text{CO}_2$  absorption of 84 different amino acid based ILs and non-functionalized ILs were elucidated using COSMO-RS and TurboMole by predicting the values of  $\text{CO}_2$  capacity, activity coefficient and Henry's constant. The results showed that amino acid-based ionic liquids as anions significantly enhanced the  $\text{CO}_2$  solubility in ILs compared to amino acid-based ionic liquids as cations. However,  $[\text{Gly}^+][\text{BF}_4]$  showed interesting  $\text{CO}_2$  capacity compared to other amino acid cations-based due to increase molecular interaction. The results showed that the selection of cations/anions combination can significantly vary the  $\text{CO}_2$  affinity of  $\text{CO}_2$  in ILs. The affinity can be governed by acid/base interaction, hydrogen bond strength, and the nonpolar-nonpolar interaction.

## Acknowledgement

This research was funded by Yayasan Universiti Teknologi PETRONAS (YUTP-FRG-015LC0-455). The authors also acknowledge technical support and facilities from the Chemical Engineering Department and Centre of Research in Ionic Liquids of Universiti Teknologi PETRONAS.

## References

- [1] N. Noorani, A. Mehrdad,  $\text{CO}_2$  solubility in some amino acid-based ionic liquids: Measurement, correlation and DFT studies, *Fluid Ph. Equilibria*. 517 (2020)112591. <https://doi.org/10.1016/j.fluid.2020.112591>
- [2] T. M. Gür, Carbon dioxide emissions, capture, storage and utilization: Review of materials, processes and technologies, *Prog. Energy Combust. Sci.* 89 (2022)100965. <https://doi.org/10.1016/j.pecs.2021.100965>
- [3] Z. Tan, S. Zhang, X. Yue, F. Zhao, F. Xi, D. Yan, H. Ling, R. Zhang, F. Tang, K. You, Attapulgitite as a cost-effective catalyst for low-energy consumption amine-based  $\text{CO}_2$  capture, *Sep. Purif. Technol.* 298 (2022)121577. <https://doi.org/10.1016/j.seppur.2022.121577>
- [4] D. Danaci, M. Bui, C. Petit, N. Mac Dowell, En route to zero emissions for power and industry with amine-based post-combustion capture, *Environ. Sci. Technol.* 55 (2021) 10619-10632. <https://doi.org/10.1021/acs.est.0c07261>
- [5] G. T. Rochelle, Amine scrubbing for  $\text{CO}_2$  capture, *Science* .359 (2009) 1652-1654. <https://doi.org/10.1126/science.1176731>
- [6] S. Zheng, S. Zeng, Y. Li, L. Bai, Y. Bai, X. Zhang, X. Liang, S. Zhang, State of the art of ionic liquid-modified adsorbents for  $\text{CO}_2$  capture and separation, *AIChE Journal*.68 (2022) 17500. <https://doi.org/10.1002/aic.17500>

- [7] C. Xu, G. Yang, D. Wu, M. Yao, C. Xing, J. Zhang, H. Zhang, F. Li, Y. Feng, S. Qi, Roadmap on ionic liquid electrolytes for energy storage devices, *Chem. Asian J.* 16 (2021) 549-562. <https://doi.org/10.1002/asia.202001414>
- [8] I. I. Sam, S. Gayathri, G. Santhosh, J. Cyriac, S. Reshmi, Exploring the possibilities of energetic ionic liquids as non-toxic hypergolic bipropellants in liquid rocket engines, *J. Mol. Liq.* 350 (2021) 118217. <https://doi.org/10.1016/j.molliq.2021.118217>
- [9] Z. Lin, Y. Su, R. Dai, G. Liu, J. Yang, W. Sheng, Y. Zhong, L. Tan, Y. Chen, Ionic liquid-induced Ostwald ripening effect for efficient and stable tin-based perovskite solar cells, *ACS Appl. Mater. Interfaces.* 13 (2021) 15420-15428. <https://doi.org/10.1021/acsami.1c01408>
- [10] Y. S. Sistla, A. Khanna, CO<sub>2</sub> absorption studies in amino acid-anion based ionic liquids, *Chem. Eng. J.* 273 (2015) 268-276. <https://doi.org/10.1016/j.cej.2014.09.043>
- [11] Y. S. Sistla, A. Khanna, Carbon dioxide absorption studies using amine-functionalized ionic liquids, *J. Ind. Eng. Chem.* 20 (2014) 2497-2509. <https://doi.org/10.1016/j.jiec.2013.10.032>
- [12] X. Zhu, Z. Chen, and H. Ai, Amine-functionalized ionic liquids for CO<sub>2</sub> capture, *J. Mol. Model.* 26 (2020) 1-12. <https://doi.org/10.1007/s00894-019-4247-5>
- [13] M. S. R. Shahrom, C. D. Wilfred, D. R. MacFarlane, R. Vijayraghavan, F. K. Chong, Amino acid based poly (ionic liquid) materials for CO<sub>2</sub> capture: effect of anion, *J. Mol. Liq.* 276 (2019) 644-652. <https://doi.org/10.1016/j.molliq.2018.12.044>
- [14] R. J. Hook, An investigation of some sterically hindered amines as potential carbon dioxide scrubbing compounds, *Ind. Eng. Chem. Res.* 36 (1997) 1779-1790. <https://doi.org/10.1021/ie9605589>
- [15] P. Kumar, J. Hogendoorn, G. Versteeg, P. Feron, Kinetics of the reaction of CO<sub>2</sub> with aqueous potassium salt of taurine and glycine, *AIChE Journal.* 49 (2003) 203-213. <https://doi.org/10.1002/aic.690490118>
- [16] P. Kumar, J. Hogendoorn, P. Feron, G. Versteeg, New absorption liquids for the removal of CO<sub>2</sub> from dilute gas streams using membrane contactors, *Chem. Eng. Sci.* 57 (2002) 1639-1651. [https://doi.org/10.1016/S0009-2509\(02\)00041-6](https://doi.org/10.1016/S0009-2509(02)00041-6)
- [17] A. Klamt, Conductor-like screening model for real solvents: a new approach to the quantitative calculation of solvation phenomena, *J. Phys. Chem.* 99 (1995) 2224-2235. <https://doi.org/10.1021/j100007a062>
- [18] A. Klamt, V. Jonas, T. Bürger, J. C. Lohrenz, Refinement and parametrization of COSMO-RS, *J. Phys. Chem A.* 102 (1998) 5074-5085. <https://doi.org/10.1021/jp980017s>
- [19] H. W. Khan, A. V. B. Reddy, M. M. E. Nasef, M. A. Bustam, M. Goto, M. Moniruzzaman, Screening of ionic liquids for the extraction of biologically active compounds using emulsion liquid membrane: COSMO-RS prediction and experiments, *J. Mol. Liq.* 309 (2020) 113122. <https://doi.org/10.1016/j.molliq.2020.113122>
- [20] E. A. Recker, M. Green, M. Soltani, D.H. Paull, G.J. McManus, J.H. Davis Jr, A. Mirjafari. Direct Air Capture of CO<sub>2</sub> via Ionic Liquids Derived from "Waste" Amino Acids," *ACS Sustainable Chemistry Engineering*, 10(2022) 11885-11890. <https://doi.org/10.1021/acssuschemeng.2c02883>